Pergamon

Chemical Engineering Science, Vol. 53, No. 1, pp. 123–130, 1998

Printed in Great Britain
PII: S0009-2509(97)00276-5
0009-2509/98 $19.00 + 0.00

Falling film hydrodynamics in slug flow

Wayez R. Ahmad, Julio M. DeJesus, Masahiro Kawaji*
Department of Chemical Engineering and Applied Chemistry, University of Toronto, Toronto, Ontario M5S 3E5, Canada

(Received 4 March 1996; accepted 6 May 1997)

Abstract—Non-intrusive flow visualization using photochromic dye activation is applied to study the near-wall region around individual and coalescing pairs of Taylor bubbles rising in stagnant kerosene in a vertical 25.6 mm ID tube. Instantaneous velocity profile measurements have been performed in the liquid film flowing past the rising Taylor bubble. A simple predictive procedure for estimating film velocity is successfully implemented. New and interesting phenomena are observed primarily in the wake region that are of significance to slug flow modeling. © 1997 Elsevier Science Ltd

Keywords: Falling film; flow visualization; slug flow; Taylor bubble.

1. INTRODUCTION

Slug flow is encountered in many practical applications such as distillation columns, gas absorption units, nuclear reactors, oil-gas pipelines, and steam boilers. In many cases, the two-phase flow occurs in vertical or horizontal flow channels, such as ducts and round pipes, over a wide range of temperatures and pressures and with or without heat transfer.

A detailed understanding of the hydrodynamics of slug flow has been difficult to obtain experimentally since the liquid film surrounding rising gas slugs is very thin (on the order of one millimeter) and thus difficult to measure without it being physically disturbed. In the present work, the photochromic dye activation method is used to make detailed instantaneous microscale measurements necessary to understand the hydrodynamics of slug flow. In the photochromic dye activation method velocity measurements and flow visualization are performed simultaneously to characterize flow structures. The application of this technique to two-phase flows is described by Kawaji *et al.* (1993).

Slug flow in vertical tubes has been investigated since the early 1940s (Campos and DeCarvalho, 1988; Collins *et al.* 1978; Davies and Taylor, 1950; Dumitrescu, 1943; Fernandes *et al.*, 1983; Mao and Dukler, 1989; Moissis and Griffith, 1992; Nicklin *et al.*, 1962; Street and Tek, 1965). In previous studies dealing with hydrodynamic modeling of the flow, there is uncertainty regarding the velocity and shear stress boundary conditions at the bubble–liquid interface (Mao and Dukler, 1991). None of the model calculations of the velocity in the liquid surrounding the bullet-shaped gas bubbles, often referred to as Taylor bubbles, have been verified by comparison with experimental results, since no quantitative velocity profile measurements have been reported to date. It should be mentioned however, that Shemer and Barnea (1987) qualitatively characterized the liquid velocity profile behind Taylor bubbles using the hydrogen bubble technique.

In the present study, velocity profiles are obtained in the liquid film and in the wake for the near-wall region surrounding single Taylor bubbles and pairs of Taylor bubbles.

2. EXPERIMENTAL APPARATUS AND METHODOLOGY

The two-phase flow loop is shown in Fig. 1. The test section was a 3.0 m long, 25.6 mm I.D. Pyrex tube that was vertically aligned to within 1 mm over its entire length. The test fluids were air and Shell-Sol 715 (deodorized kerosene) with 0.01% concentration of photochromic dye 1,3,3 trimethylindoline-6-nitrobenzospiropyran. This concentration provided sharp traces in the liquid upon excitation that penetrated more than half the test section diameter.

Taylor bubbles were produced in a 3.0 m long, 25.6 mm ID flexible developing flow section connected to the test section inlet and consisting of a horizontal tube followed by a long, gradually inclined bend. Taylor bubble size and frequency were controlled using a combination of a metering valve and a solenoid valve. Bubbles were formed in the horizontal leg of the developing flow section. A small jack was used to adjust the angle of inclination of the developing flow section, thereby minimizing disturbances to the liquid phase. Sufficient interphase contacting before air injection was used to minimize mass transfer effects.

*Corresponding author.

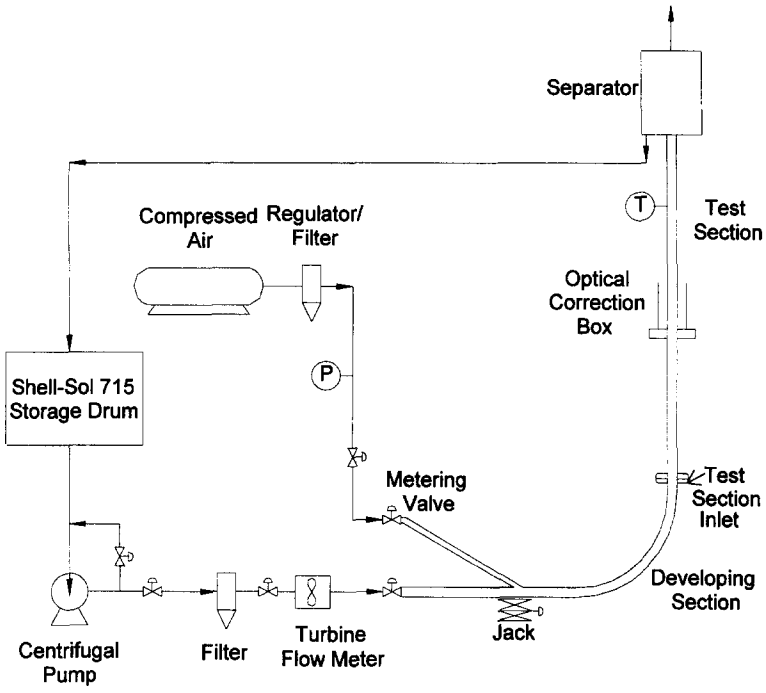

Fig. 1. Experimental flow loop.

A 351 nm wavelength ultraviolet beam was produced by a commercially available excimer laser and passed through a collimating slit into an array of four lenses, each of 250 mm focal length. The lens array served to further divide and focus the beam into four traces spaced 2 mm apart. The distance between the lens array and the test section was kept large compared to the diameter of the test section so that nearly cylindrical traces with small divergence were produced. An optical correction box filled with dye-free kerosene was used to correct for optical distortion near the circular wall of the test section. Linearity of the distance observed with the video camera was checked in a separate experiment by inserting a needle on the inside of the tube and measuring the distance between the tip and the inner tube wall.

Taylor bubble rise velocities were measured using two synchronized video cameras mounted at elevations of 87 and 234 cm from the test section inlet. The trace sequences were recorded using a high speed digital video camera mounted at the 198 cm elevation. For the present work a rectangular view field of 32×256 pixels corresponded to a 3.0 mm frame size in the minimum pixel direction. The camera frame rate was set at 1488 frames per second at a shutter speed of 5 kHz. The high shutter speed required adequate background lighting that was provided by a 1 kW sodium lamp.

Images were captured for analysis on a personal computer using commercially available image analysis software. The digitized traces were processed to obtain velocity profiles in the liquid film surrounding Taylor bubbles.

Two sets of experiments were performed with stagnant liquid capturing 52 single Taylor bubbles ranging in size from 2.9 to 11.8 cm and 36 pairs of Taylor bubbles with leading slugs of 2.6 to 2.9 cm length followed by trailing slugs of 6.7 to 7.6 cm length. For the two bubble experiments, the injection spacing between successive Taylor bubbles was adjusted so that coalescence would occur within the test section above the visualization window.

3. FLOW VISUALIZATION

Before discussing the velocity data, it is pertinent to obtain a visual perspective of the actual flow and laser induced dye trace motion. To this end, representative photographic sequences are shown in Figs 2–4. These pictures were obtained by the frame grabber from the videotapes. Successive still frames cannot easily convey dynamic information, however, they show some new and very interesting features of the flow. The emphasis of this discussion is on the liquid film dynamics in the wake region. Flow visualization near the nose has been described in a separate paper by Kawaji *et al.* (1993).

Since the video camera was mounted sideways to increase the length of the viewing window the positive upward direction is to the right of the figures and the top line corresponds to the inner wall of the test section. The distance from the wall to the lower edge of the frames is 3.0 mm. When present, Taylor bubbles appear as the dark structure on the lower right side of the images. The times shown in the windows are used to illustrate the relative succession of frames and do not correspond to the initial laser firing.

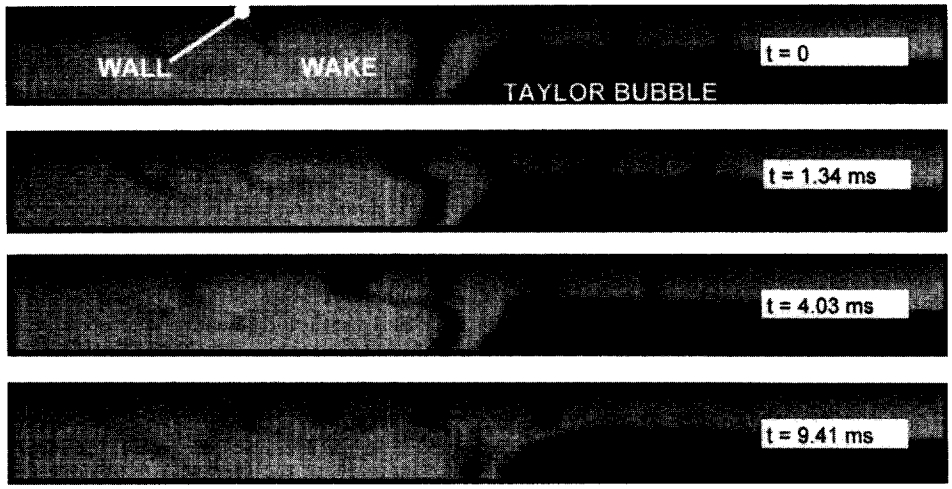

Fig. 2. Flow visualization at the tail of a 3 cm Taylor bubble.

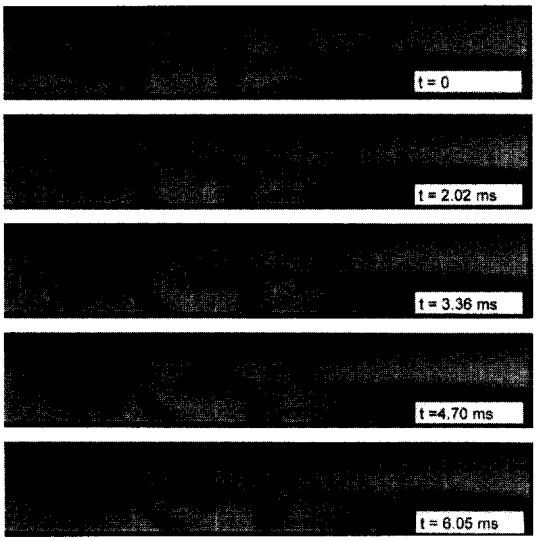

Fig. 3. Production of vortices in the near-wake of a 3 cm Taylor bubble.

Close inspection of Fig. 2 reveals that there is no evidence of interfacial shear stress. The falling film is seen penetrating into the wake creating a mixing zone. Furthermore, the sequence of images shows a clear upward movement of liquid in the near-wall region behind the rising Taylor bubble, and thus a strongly sheared layer at the film/core boundary. The images show a falling film that is clearly delineated from the bulk fluid.

Accumulation of dyed fluid on the Taylor bubble surface leads to the formation of a thin interfacial layer that is very useful in identification of qualitative features of the wake. For example, Fig. 3 shows the dye layer continuing to follow the shape of the bubble past its tail, thereby clearly identifying the film/core interface. As expected, a fluid shear layer is clearly visible. The leftmost laser trace shows dramatic footage of the development and dynamics of a vortex formed near the wall region of the test section. Strong mixing of the liquid between the film and the core is shown in the last two photographs of this sequence. This vortex increases in size and in so doing touches the wall, breaking up the continuous film. The last picture shows rapid dispersion of the dye layer by a swirling motion in the wake.

Figure 4 is taken from a two bubble experiment where coalescence would occur just above the viewing window. In the first image, the Taylor bubble surface is violently distorted by large waves that travel down the side of the bubble, unlike the smooth interface

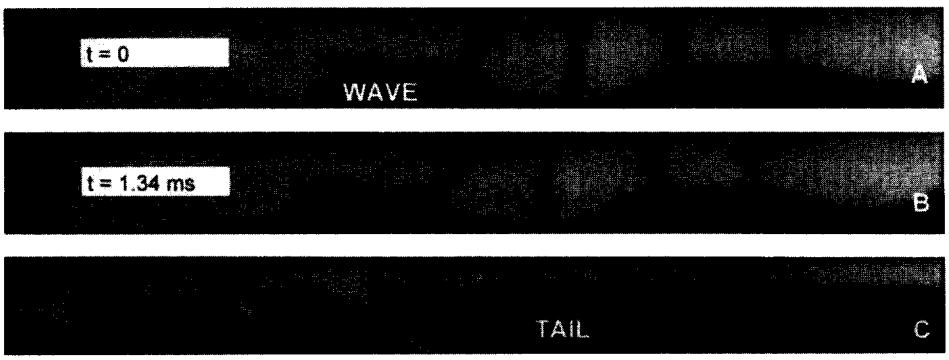

Fig. 4. Trailing Taylor bubble in a two bubble system: A, B during and C immediately after coalescence.

seen previously. These waves may cause lateral motion of the Taylor bubble, which is alternately pushed side to side changing the film thickness. During this process large amplitude (~ 0.3 mm) waves travel down the interface causing extensive shearing of the tail. This wavy motion dissipates within approximately 10 ms of bubble coalescence resulting in the smooth interface shown in the last image. The Taylor bubble then rises very smoothly, albeit with a bubbly swarm in its wake. Additional observations have shown that this bubble rapidly acquires the rise velocity of a single bubble. Prior to coalescence, trailing Taylor bubbles in two bubble systems had greater rise velocities that were inversely related to the bubble separation distance. This confirms that trailing Taylor bubbles were affected by the wake or its effects behind the leading bubble causing faster rise and eventual coalescence. A mechanism for coalescence has been postulated by DeJesus *et al.* (1995).

4. VELOCITY PROFILES

To indicate the location where the velocity profiles are measured, the following convention is used: axial distances are referenced to the bubble nose and are negative ahead of, and positive below the Taylor bubble nose. On the other hand, velocities are based on an Eulerian frame of reference and are positive in the upward direction.

4.1. *Radial profiles of axially averaged velocity*

The near-wall velocities were axially averaged over a 2 mm distance, to show radial profiles of liquid velocity. Figs 5–7 correspond to single bubble experiments and Figs 8 and 9 are for two bubble experiments. The figures show film velocity as a function of distance from the wall at different axial distances, x, for both bubble and wake regions.

4.1.1. *Bubble region.* In the bubble region, the upper half of Figs 5–7 show similar trends. Near the nose and ahead of the Taylor bubble the film velocity is zero. Therefore, flow reversal is first seen around the nose and the liquid ahead of the nose is essentially unaffected by the rising Taylor bubble. Velocities then increase with decreasing film thickness (or equivalently increasing axial distance from the nose). The fluid velocities are all negative (downward flow) and they increase for the 11.5 cm Taylor bubble from 0 to 1.4 m/s as the film thickness decreases from 12.7 to 0.7 mm.

Reliable wall shear stress data could not be obtained due to optical effects and lower than required high speed video camera resolution. In this high shear region near the tube wall, the traces are stretched near the wall to a thickness less than the minimum observable pixel size. However, the figures suggest considerable wall shear stress, since the velocity reaches a fairly uniform value within approximately 0.2 mm of the wall. The traces extend to the Taylor bubble interface on the right side of the figure and consistently show only slight deviations from linearity at the interface. This suggests that the interfacial shear, if any, is immeasurably small. Any apparent interfacial shear is likely due to the small

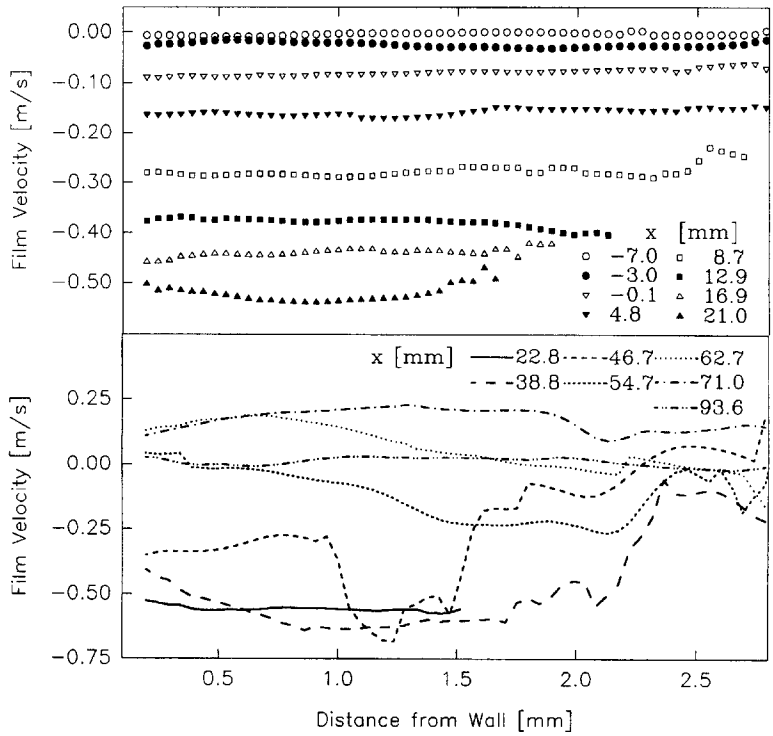

Fig. 5. Axially averaged velocity profiles for a 3 cm Taylor bubble.

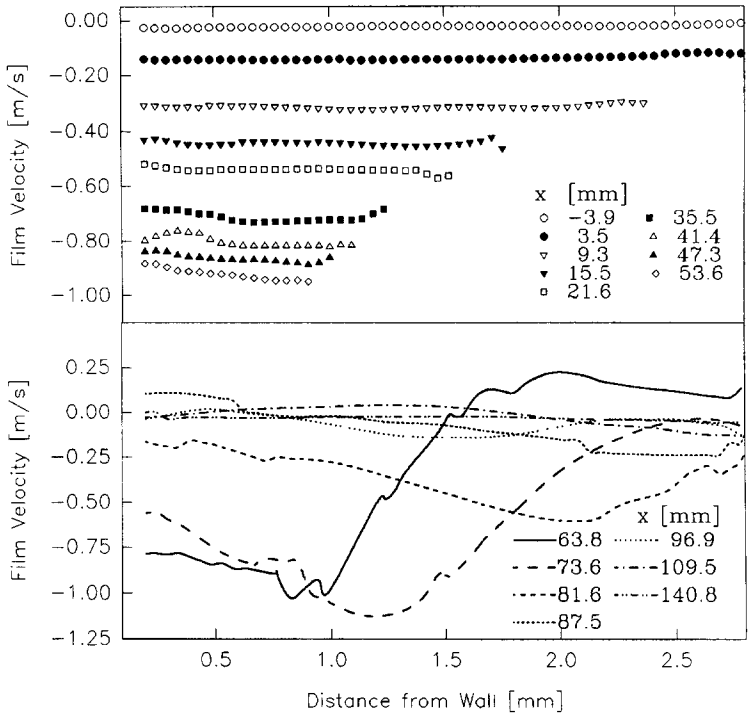

Fig. 6. Axially averaged velocity profiles for a 6 cm Taylor bubble.

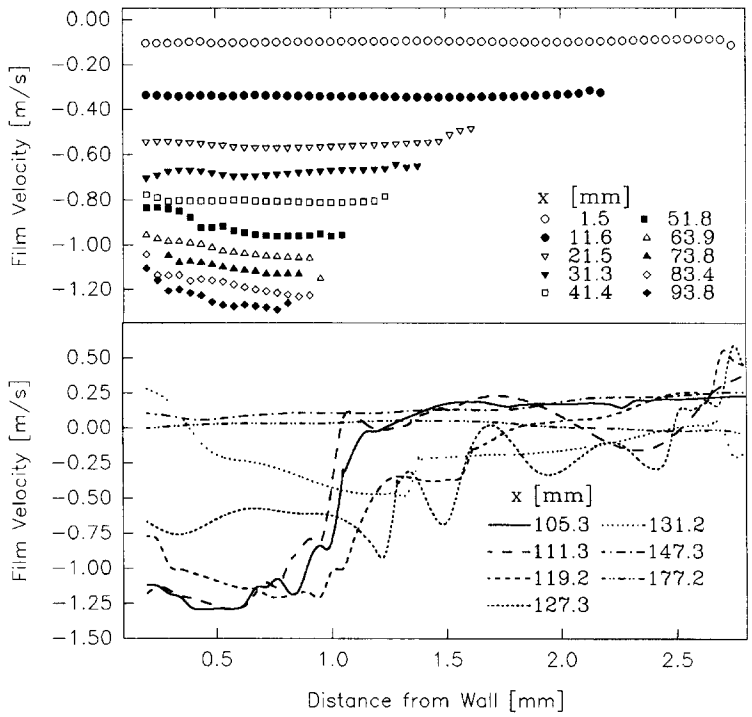

Fig. 7. Axially averaged velocity profiles for an 11.5 cm Taylor bubble.

sample size (typically about four) used for velocity digitization.

The flat velocity profile near the nose indicates free falling liquid in the initial stages of film formation. Further down in the film the velocity profiles imply boundary-layer development, for example, in Fig. 7. Further still ($x > 60$ mm), the velocity profile is characteristic of developing falling film flow, that is the

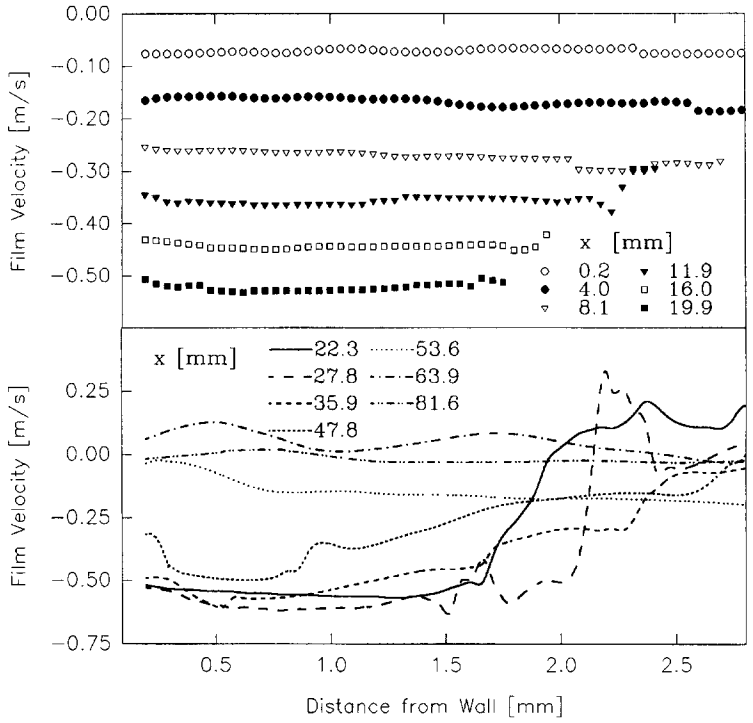

Fig. 8. Axially averaged velocity profiles for a 3 cm leading Taylor bubble in a two-bubble system.

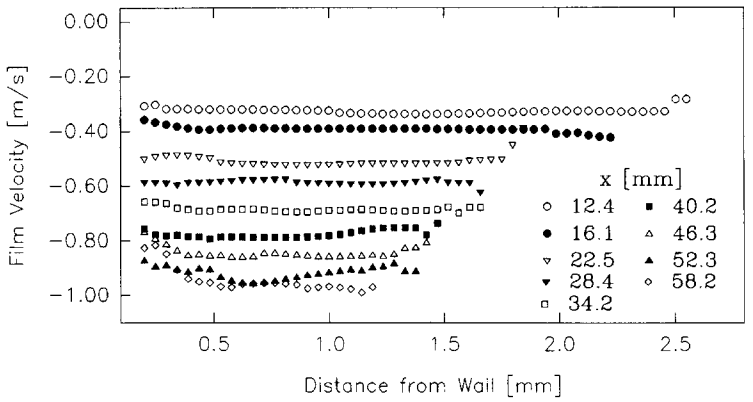

Fig. 9. Axially averaged velocity profiles for a 6 cm trailing Taylor bubble in a two-bubble system.

film velocity is higher near the interface than close to the pipe wall.

Figure 8 shows the data for the leading bubble in a two bubble system. The velocity profile in the bubble region is very similar to Fig. 5. Hence, it appears that trailing bubbles have very little effect on the leading bubble, at least until coalescence. Figs 6 and 9 depict the velocity profile for similar bubble sizes (6 cm). Figure 6 is for a single bubble run and Fig. 9 is for the trailing bubble in a two bubble case. Careful observation shows that the velocity profiles are similar for distances greater than 2 cm below the nose. Although velocity data at the nose could not be obtained for the trailing Taylor bubble, the velocities between 0.9 and 1.6 cm below the nose are slightly greater for the single bubble case than the two bubble case. This apparent difference may be explained from a qualitative viewpoint. Visual observations and the film velocity data in the wake, to be discussed next, show that when the falling film ceases to penetrate the bulk liquid in the wake, the liquid near the wall rises before it begins to settle again with some residual eddies. If a trailing bubble nose is present when this happens, then the net downward velocity of the film near the nose would be less than if the flow were stagnant as is the case for the single bubble experiments. This would make the initial condition in the liquid, as seen by the trailing Taylor bubble, different

compared to that for a leading or single Taylor bubble.

4.1.2. *Wake region.* The radial profiles of axial velocity in the wake region are shown in the lower half of Figs 5–9. In the near-wake, the falling liquid film is clearly seen close to the wall. Further below the tail of the Taylor bubble, the film thickness increases and consequently, the film velocity decreases. Also, as expected, the velocity profiles are very wavy near the tail, e.g. Fig. 7 at $x = 111.3$ mm. This is due to the vortex motion previously discussed. There is no evidence suggesting that the film continues to accelerate past the tail and penetrate deep into the wake. In all the runs examined in this work, the liquid film begins to decelerate when it flows past the Taylor bubble and enters the wake. There are periods where the entire flow near the wall is upwards, perhaps due to the three-dimensional flow in the wake or because of downward flowing liquid outside the viewing window in the core of the pipe.

The waviness of the velocity profile increases for the longer bubbles. This could be due to two factors. For longer Taylor bubbles, the falling film has a higher velocity when it enters the wake so that there is greater shear between the film and rising near-wall liquid core as evidenced by the steeper slope of Fig. 7 at $x = 105.3$ mm compared to that of Fig. 6 at $x = 63.8$ mm. Alternatively, it may be due to shearing and entrainment of small bubbles at the Taylor bubble tail, which enhances mixing in the wake. Our observations suggest that the critical film velocity that causes shearing and bubble entrainment appears is approximately 1 m/s. Far downstream, the liquid velocity profile is essentially flat as vortices decay, e.g. Fig. 7 at $x = 177.2$ mm.

4.2. *Radially averaged velocity profiles*

The shape and rise velocity of a Taylor bubble can be used to predict the radially averaged velocity profile in the liquid film, $U_f(x)$, since by continuity

$$Q = U_{TB}A = \int_{A_f} U^*(x)\,dA = (U_f(x) + U_{TB})A_f \tag{1}$$

where U_{TB} is the Taylor bubble rise velocity and U^* is the relative film velocity in the coordinate system moving with the bubble nose. Hence, the radially averaged velocity at any axial position along the Taylor bubble can be predicted from the measured film thickness, $\delta(x)$, by rearranging eq. (1):

$$U_f = \frac{U_{TB}A}{A_f} - U_{TB}$$

$$= \frac{U_{TB}\pi D^2/4}{\pi\delta(D-\delta)} - U_{TB}. \tag{2}$$

Figure 10 shows the measured average film velocity profile and the predicted film velocities along the Taylor bubble. A second prediction based on the film thickness profile of Dumitrescu (1943) is also shown. The results for this and other runs are very consistent and the prediction of film velocity is excellent using

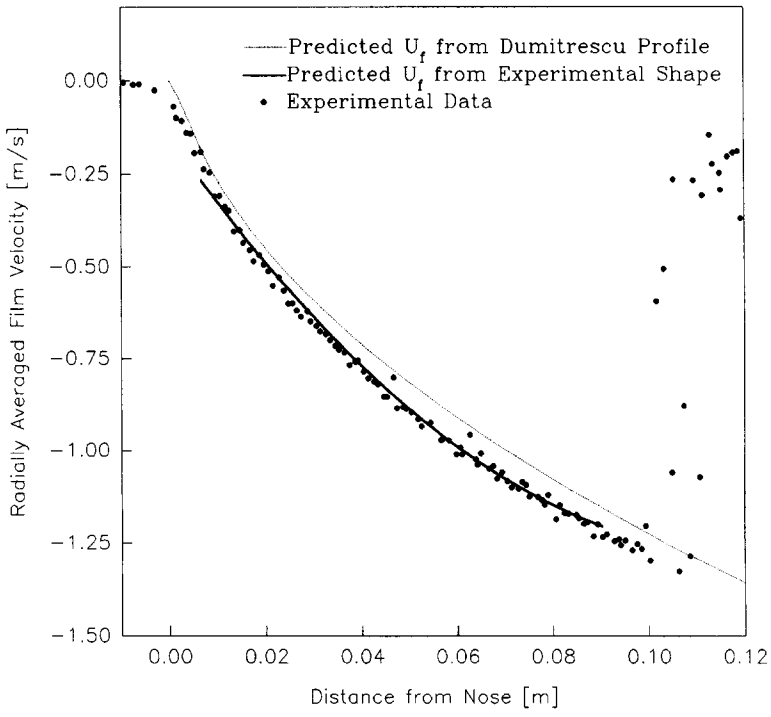

Fig. 10. Experimental and predicted radially averaged velocity profiles.

either the Dumitrescu or experimental bubble shape profile. This establishes both the accuracy and reproducibility of the velocity data along the Taylor bubble. Furthermore, the one-dimensional assumption used in calculating the velocities along the bubble appears valid.

4.2.1. *Bubble region.* The slope of the velocity profile in Fig. 10 shows greater liquid acceleration near the nose. In this region, the film thickness decreases rapidly. Liquid continuity dictates a rapid downward flow to accommodate the rise of the Taylor bubble. For the longest Taylor bubble tested (11.5 cm) the film velocity continues to increase without reaching a terminal velocity, however, the Taylor bubble lengths studied are insufficient to conclude whether or not a terminal velocity would eventually be reached in the liquid film for a sufficiently long Taylor bubble. The slight scatter of the velocity data further downstream is possibly due to a growing boundary layer. At the tail of the Taylor bubble, the range of velocities increases dramatically.

4.2.2 *Wake region.* The radial velocity data in the wake region is only approximate since swirling vortices create a three-dimensional flow field. Furthermore, random fluid motion in the wake causes larger deviations of the velocity than in the film around the Taylor bubble. It is however, readily apparent that approximately two tube diameters behind the Taylor bubble tail, large vortices have dramatically decayed and the flow tends to the stagnant condition again.

5. CONCLUSIONS

Experimental investigation of vertical slug flow in a 25.6 mm ID tube using photochromic dye activation in conjunction with digital, high-speed video photography and image analysis provided qualitative and quantitative data for characterizing the hydrodynamics of idealized slug flow of single and dual Taylor bubbles in stagnant liquid.

The results show that the velocity profiles in the liquid along the Taylor bubble are initially flat but eventually assume the characteristic shape for boundary-layer development. No interfacial shear was observed. Liquid velocities near the nose for a trailing Taylor bubble are slightly less than those for a solitary gas slug. Furthermore, the trailing Taylor bubble had an immeasurable effect on the near-wall liquid velocity of the lead bubble.

The radially averaged velocity profiles could be accurately predicted using the Dumitrescu shape profile, thereby confirming that the flow in the liquid film is essentially one-dimensional and nearly inviscid along the Taylor bubble just below the nose.

For film velocities slightly greater than 1 m/s shearing occurred at the Taylor bubble tail. In all cases, the falling liquid film decelerated immediately below the Taylor bubble tail.

In the near-wake region just below the tail, the deviations in the velocity data were many times greater than those in the film above the tail. However, in the far-wake the rapid decay of vortices reduced these deviations in velocity and the liquid near the wall returned rapidly to a stagnant state.

NOTATION

A	cross-sectional area, m^2
D	tube diameter, m
U	velocity, m/s
x	axial distance, m

Greek letters

δ	film thickness, m

Subscripts and superscripts

*	coordinate system moving with the bubble nose
f	film
TB	Taylor bubble

REFERENCES

Kawaji, M., Ahmad, W., DeJesus, J. M., Sutharshan, B., Lorencez, C. and Ojha, M. (1993) *Nucl. Engrs Des.* **141**, 343.

Campos, J. B. L. M. and DeCarvalho, J. R. F. G. (1988) *J. Fluid Mech.* **196**, 27.

Collins, R., DeMoraes, F. F., Davidson, J. F. and Harrison, D. (1978) *J. Fluid Mech.* **89**, 497.

Davies, R. M. and Taylor, G. I. (1950) *Proc. Roy. Soc. London Ser. A* **200**, 375.

Dumitrescu, D. T. (1943) *ZAMM* **23**, 139.

Fernandes, R. C., Semiat, R. and Dukler, A. E. (1983) *A.I.Ch.E. J.* **29**, 981.

Mao, Z. S. and Dukler, A. E. (1989) *Exp. Fluids* **8**, 169.

Moissis, R. and Griffith, P. (1992) *J. Heat Transfer* **84**, 29.

Nicklin, D. J., Wilkes, J. O. and Davidson, J. F. (1962) *Trans. Instn Chem. Engrs* **40**, 61.

Street, J. R. and Tek, M. R. (1965) *A.I.Ch.E. J.* **11**, 644.

Mao, Z. S. and Dukler, A. E. (1991) *Chem. Engng Sci.* **46**, 2055.

Shemer, L. and Barnea, D. (1987) *PhysicoChem. Hydrodynam.* **8**, 243.

DeJesus, J. M., Ahmad, W. R. and Kawaji, M. (1995) *Advances in Multiphase Flow*, eds A. Serizawa, T. Fukano and J. Bataille. Elsevier, Amsterdam.